



HAL
open science

Fluorescence microscopy and photodielectric characterization studies of the composite films of polyvinyl alcohol and tryptophan functionalized silver nanoparticles

Dušan K Božanić, Radovan Dojčilović, Jelena D Pajović, Dragana Tošić,
Duško Dudić, Matthieu Réfrégiers, Vladimir Djoković

► To cite this version:

Dušan K Božanić, Radovan Dojčilović, Jelena D Pajović, Dragana Tošić, Duško Dudić, et al.. Fluorescence microscopy and photodielectric characterization studies of the composite films of polyvinyl alcohol and tryptophan functionalized silver nanoparticles. *Colloids and Surfaces A: Physicochemical and Engineering Aspects*, 2022, 634, pp.128050. 10.1016/j.colsurfa.2021.128050 . hal-03468262

HAL Id: hal-03468262

<https://hal.science/hal-03468262>

Submitted on 7 Dec 2021

HAL is a multi-disciplinary open access archive for the deposit and dissemination of scientific research documents, whether they are published or not. The documents may come from teaching and research institutions in France or abroad, or from public or private research centers.

L'archive ouverte pluridisciplinaire **HAL**, est destinée au dépôt et à la diffusion de documents scientifiques de niveau recherche, publiés ou non, émanant des établissements d'enseignement et de recherche français ou étrangers, des laboratoires publics ou privés.

Fluorescence microscopy and photodielectric characterization studies of the composite films of polyvinyl alcohol and tryptophan functionalized silver nanoparticles

Dušan K. Božanić¹, Radovan Dojčilović¹, Jelena D. Pajović², Dragana Tošić¹, Duško Dudić¹

Matthieu Réfrégiers^{3,4}, Vladimir Djoković^{1*}

¹*Vinča Institute of Nuclear Sciences, National Institute of the Republic of Serbia, University of Belgrade, P.O. Box 522, 11001 Belgrade, Serbia*

²*Faculty of Physics, University of Belgrade, P. O. Box 368, 11001 Belgrade, Serbia*

³*DISCO Beamline, Synchrotron SOLEIL, F-91192 Gif sur Yvette, France*

⁴*Centre de Biophysique Moléculaire, CNRS UPR4301, Rue Charles Sadron, 45071 Orléans, France*

Abstract

Fluorescent nanocomposite films were prepared by solution mixing of polyvinyl alcohol (PVA) and tryptophan amino acid functionalized silver (AgTrp) nanoparticles. Tryptophan absorbs in the UV part of the electromagnetic spectrum and the synchrotron excitation deep-ultraviolet (DUV) fluorescence imaging was used to follow the distribution of AgTrp nanoparticles within the polymer matrix. The study showed changes in the PVA morphology after its mixing with AgTrp and pure tryptophan (the pure and hybrid PVA-tryptophan films are used as reference materials). Pronounced growth of dendrite-like structures in the presence of AgTrp nanoparticles was confirmed by bright field and fluorescence imaging as well as with atomic force microscopies. Also, the fluorescent imaging revealed that the nanoparticles are localized at the boundaries between dendritic structures and the amorphous parts of the polymer. Both tryptophan and AgTrp nanoparticles influence the thermal properties of the host matrix. Differential scanning calorimetry (DSC) measurements showed that they reduce crystallinity and significantly increase the glass transition temperature of PVA (in the case of PVA-AgTrp film the T_g increases by ~ 20 °C). Tryptophan and the nanoparticles slightly affect the thermal decomposition route of the matrix leading to the changes in the carbonization stage at the end of the degradation process. The dielectric properties of the films were studied under two different conditions (dark and illumination). It was found that illumination with 250 nm light induces a significant increase in conductance of PVA-AgTrp nanocomposite. The relative changes, with respect to the conductance measured in the dark, were almost $\sim 200\%$.

*Corresponding author: djokovic@vin.bg.ac.rs

1. Introduction

Polymer nanocomposites based on polyvinyl alcohol (PVA) as matrix material are among the most studied systems [1,2]. PVA is considered to be a good host for nanostructured fillers due to easy processability, thermo-stability and chemical resistance. It is biologically friendly, water-soluble, polymer suitable for medical and packaging applications [3]. PVA has good chelation properties and may act as both a reducing agent and a stabilizer for metallic nanoparticles [4]. For these reasons, it has been extensively used as a matrix for nanoparticles of noble metals such as Au [5-7], Ag [7-16], Cu [8], Pt [17]. PVA-noble metal nanocomposites are especially interesting for optical applications [5-11], but they have been also employed for sensing [12], as thin film capacitors [13] and for catalysis [17]. In addition, PVA-Ag nanocomposites exhibit antimicrobial properties due to the potent activity of silver nanoparticles against gram-negative and gram-positive bacteria [11,15,16]. On the other hand, metallic nanoparticles may influence the PVA matrix to a high extent leading to interesting properties of the resulting composite material. For example, we showed that the addition of low amounts of silver nanoparticles (less than 1 wt.%) could double the mechanical strength of the PVA film and induce an increase in its glass transition temperature of ~ 20 °C [14]. In the present study, we will investigate the nanocomposites of PVA and tryptophan functionalized silver (AgTrp) nanoparticles.

Recently, we created a fluorescent nano-probe for bioimaging of microbial cells by surface modification of Ag and Au nanoparticles with the amino acid tryptophan [18-19]. It was shown that the fluorescence of the obtained nanoparticles depends on the environment they are embedded in. Changing the surroundings of the nanoparticles from polar to non-polar induced a blue shift of the fluorescence towards lower wavelengths. Here, we will try to exploit further these optical properties and study their interaction with PVA. Having nanoparticles with additional functionality, e.g. fluorescence, opens the possibility to study their dispersion within the PVA matrix by means of fluorescence microscopy. Since tryptophan absorbs in the UV part of the optical spectrum, we used synchrotron deep-UV radiation as an excitation source. The changes in the morphology of PVA after the introduction of AgTrp particles were studied on the TELEMOS fluorescent microscope at the DISCO beamline of synchrotron SOLEIL. Finally, we report on thermal, dielectric and photodielectric properties of the hybrid PVA films.

2. Experimental

2.1. Materials

Polyvinyl alcohol ($M_w = 72\,000\text{ g mol}^{-1}$, degree of hydrolysis ~98%) was purchased from Merck. Sodium borohydride (NaBH_4), silver nitrate (AgNO_3), sodium hydroxide (NaOH) and tryptophan (Trp) were products of Sigma-Aldrich, used as received. High purity water with specific resistance $\sim 10^{18}\ \Omega\text{m}$ was used in all synthetic procedures.

2.2. Synthesis of tryptophan functionalized silver nanoparticles

Silver colloids (Ag NP) and colloids of tryptophan functionalized silver nanoparticles (AgTrp) in water were prepared according to the procedure published elsewhere [18]. The silver nanoparticles were prepared by reduction of silver nitrate with NaBH_4 . Prior to the functionalization of the silver nanoparticles, the pH value of the hydrocolloid was adjusted to 10.4. Functionalization of the nanoparticles was carried out by adding an appropriate amount of tryptophan (Ag:Trp molar ratio 1:1).

2.3. Fabrication of PVA nanocomposite films

PVA water solution (5%) was mixed with appropriate amounts of Ag and AgTrp hydrocolloids as well as with pure tryptophan solution. The mixtures were poured into plastic Petri dishes, and the hybrid films were obtained after drying at $30\text{ }^\circ\text{C}$ for 24 h under a controlled humidity of 37%. The thickness of the obtained films was $\sim 70\ \mu\text{m}$. For the microscopy measurements, the films were much thinner ($\sim 10\ \mu\text{m}$) and they were prepared by deposition of the mixtures on quartz holders, transparent to ultraviolet.

2.4 Experimental methods

The UV–vis absorption spectroscopy measurements of the aqueous dispersions and hybrid films were carried out on a Thermo Evolution 600 spectrophotometer.

FTIR spectroscopy of the pure PVA and hybrid PVA films was carried out at room temperature using a Nicolet 380 spectrophotometer in the spectral range of $4000\text{--}400\text{ cm}^{-1}$.

The photoluminescence spectra of aqueous tryptophan solution and AgTrp colloids as well as PVA hybrid films were recorded by using a PerkinElmer LS45 fluorescence spectrophotometer.

Surface morphologies of the neat PVA and hybrid PVA films were investigated by atomic force microscopy (AFM, Quesant micro-scope, Ambios Technology). Samples were deposited on a mica surface and dried in air, at room temperature. The measurements were performed in air, using standard silicon Q-WM300 probes with a spring constant of 40 Nm^{-1} . All images were obtained in tapping mode over different square areas at 2 Hz scan rate.

Synchrotron DUV fluorescence microscopy measurements of PVA and hybrid PVA films were carried out at the DISCO beamline of the SOLEIL synchrotron facility (France). The fluorescence images were collected on the TELEMOS endstation of DISCO by acquiring the luminescence signals in the [327–353 nm] and [370–410 nm] wavelength ranges for 10 seconds upon illumination of the samples with $\lambda_{\text{exc}} = 250 \text{ nm}$ synchrotron radiation. To avoid the effects of photobleaching on the intensity of the fluorescence signal and to ensure the consistency of the observations, each sample was measured on at least 6 different locations ($150 \times 75 \mu\text{m}$). The images were collected through a $40\times$ ultrafluar objective (Zeiss, Germany). Under these conditions, the pixel size on the fluorescence images projected on the camera chip of a PIXIS 1024 BUV camera (Princeton, USA) corresponds to 313 nm. The images were analyzed by using FIJI software [Ref: Schindelin J, Arganda-Carreras I, Frise E, Kaynig V, Longair M, Pietzsch T, Preibisch S, Rueden C, Saalfeld S, Schmid B, Tinevez J-Y, White DJ, Hartenstein V, Eliceiri K, Tomancak P, Cardona A: Fiji: an open-source platform for biological-image analysis. Nat Methods 2012, 9:676–682.].

Differential scanning calorimetry measurements were recorded on a Setaram DSC 151R (Setaram, ??). The films were heated from 30 to 240 °C at $10 \text{ C}\cdot\text{min}^{-1}$ under a nitrogen atmosphere.

The thermogravimetric analysis (Perkin Elmer STA 6000) of the neat PVA and hybrid PVA samples was carried out under a nitrogen atmosphere in the temperature range from 50 to 800 °C. The heating rate was $10 \text{ }^\circ\text{C}\cdot\text{min}^{-1}$.

Dielectric measurements were performed on an Agilent 4284a instrument in the frequency range between 22 Hz and 600 kHz ($U_0 = 2 \text{ V}$) at room temperature ($22 \pm 0.2 \text{ }^\circ\text{C}$) and 55% relative humidity. The parallel mode of measurements (C_p) was used and the AC conductivity (admittance) is presented as $Y = G + iB$ (G - conductance and B - susceptance). The

standard LED (385 nm) and a Philips TUV G8T5 (250 nm, UV output 2.4 W) lamp were used to illuminate the samples during photodielectric measurements. The irradiances on the samples were 4.4 mW/cm^2 and 1.3 mW/cm^2 for 385 nm and 250 nm incident lights, respectively.

For the bulk dielectric measurements (performed in the dark), self-adhesive Al electrodes ($20 \times 20 \text{ mm}$) with electrically conductive adhesive were applied to the samples on both sides of the film (the photo of the sample is shown in the [Supporting information](#) Figure S1). Surface dielectric measurements under argon atmosphere were used to study the photodielectric properties of the films. For these studies, two parallel Al electrodes ($3 \times 43 \text{ mm}$) were applied on one side of the film, the mean distance between the electrodes was 1 mm. The surface of the film under test was $1 \times 43 \text{ mm}$. The samples were mounted on a $8 \times 43 \text{ mm}$ polyethylene plate. Both dielectric and photodielectric measurements were performed by using the experimental chamber specifically designed for these purposes. Figure S2 ([Supporting information](#)) shows a picture of the chamber with a sample prepared for photodielectric studies. The base line was recorded with the same sample after removing the part of the film situated between the electrodes. Photodielectric measurements were performed at a single frequency and consisted of 3 “light off” and 2 “light on” steps. The duration of each step was 25 s, while the admittance was recorded every 5 s (a total of 25 points were acquired). The relative conductivity changes (ΔG or ΔB) induced by illumination were calculated based on the mean values of conductance (G) and susceptance (B) obtained in the dark-light steps according to the following formula:

$$\Delta G = \frac{G_i - G_0}{G_0} [\%], \quad (1)$$

where G_i is the mean value of the conductance recorded during the illumination at a single frequency and G_0 is the conductance of the same sample recorded in the dark under the same conditions.

3. Result and discussion

In our previous study [18], we prepared a detailed morphological study of the bare (Ag) and tryptophan modified silver nanoparticles. For this reason, we will omit these results from the present study. Briefly, transmission electron microscopy (TEM) analysis showed that the average size of as prepared silver nanoparticles is around 6 nm. After the addition of tryptophan, their average size increases up to 10 nm. The surface modification provided a novel optical, e.g. emission, property to the silver nanoparticles. We will first consider possible changes in optical

properties after mixing the nanoparticles with PVA. After that, we will present the results on optical, morphological and thermal properties of PVA hybrid films.

3.1 Optical properties

Absorption spectra of the Ag and AgTrp hydrocolloids as well as of their mixtures with 5% water solution of PVA are shown in Figure 1a. For comparison purpose, the absorption spectra of the pure PVA and the pure tryptophan solutions are also included. The spectrum of the bare silver nanoparticles exhibits a typical surface plasmon resonance (SPR) peak at 382 nm. After the addition of the PVA, the SPR peak shifts to higher wavelengths (~401 nm) due to the formation of the polymer dielectric layer on the surface of the nanoparticles [20]. On the other hand, the absorption spectrum of AgTrp exhibits two peaks. The first peak is related to the SPR of the nanoparticles and the second appears due to agglomeration of the nanoparticles in the presence of tryptophan [18]. The tryptophan covers the surface of the AgTrp nanoparticles and the addition of the PVA solution does not affect their absorption. As can be seen in Figure 1a, the spectra of AgTrp and PVA-AgTrp solutions are virtually identical.

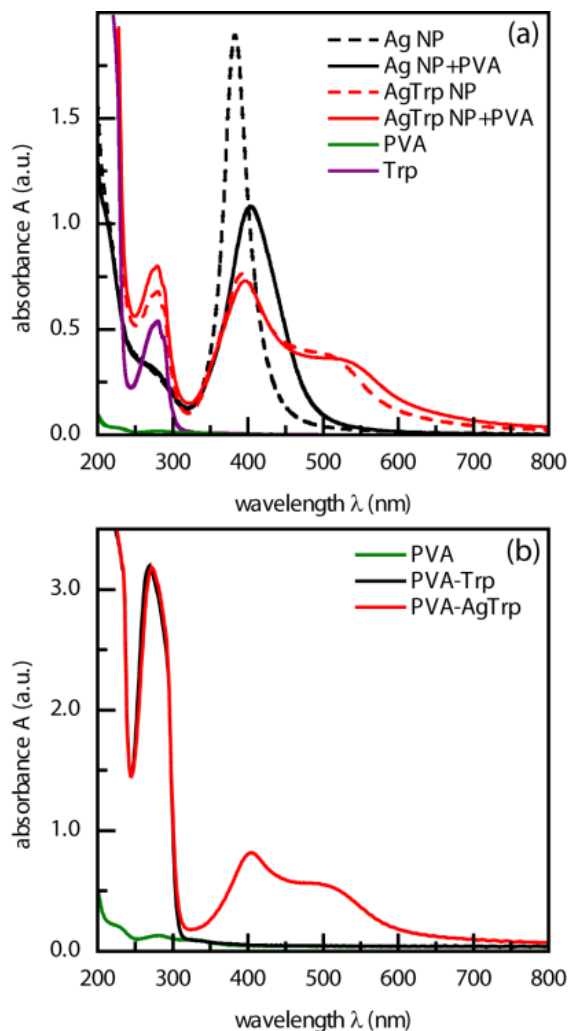


Figure 1. a) Absorption spectra of Ag and AgTrp hydrocolloids and their mixtures with 5% water solution of PVA (the spectra of the water solutions of the pure PVA and pure tryptophan are included as references). b) Absorption spectra of PVA, PVA-Trp and PVA-AgTrp films.

Figure 1b shows the absorption spectra of the pure PVA, PVA-Trp and PVA-AgTrp films. The casting of the solutions into films did not significantly affect the absorption spectra. The absorption peaks that originate from AgTrp nanoparticles are broader but observable in the spectra of the nanocomposites. The emission spectra of the PVA-AgTrp nanocomposite and PVA-Trp films obtained after excitation with $\lambda_{exc}=280$ nm light are shown in Figure 2. In the inset of Figure 2, we included the emission spectra of the water solutions of the pure tryptophan and AgTrp hydrocolloid. The emission properties of the tryptophan are preserved after incorporation into the films. Similar results are reported by Ambrosio et al. [21], who prepared fluorescent polyvinyl alcohol-polyvinyl acetate (PVA-PVAc) microspheres *via* introducing

Rhodamine dye. With respect to the spectra of the Trp and AgTrp water solutions, the spectra of the emission maxima of the hybrid PVA-Trp and PVA-AgTrp films are slightly shifted towards lower wavelengths due to the lower polarity of the PVA. The intensity of the emission of the PVA-Trp film is higher than that of the PVA-AgTrp nanocomposite due to partial fluorescence quenching induced by silver nanoparticles (both films are prepared with an equal amount of tryptophan relative to PVA).

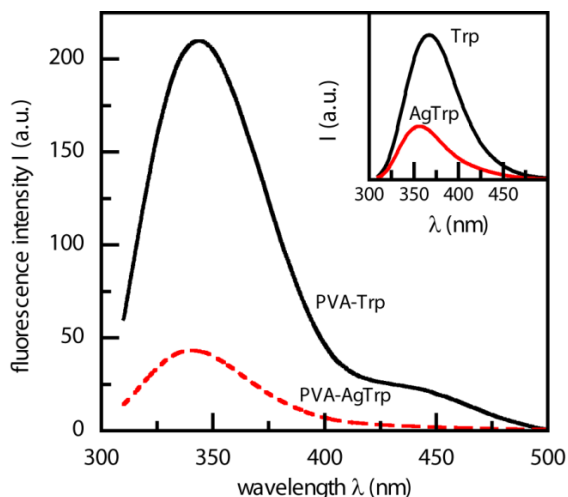


Figure 2. PL emission spectra of PVA-AgTrp nanocomposite and PVA-Trp films. The excitation wavelength was 280 nm. Inset shows the emission spectra of the water solutions of the pure tryptophan and AgTrp hydrocolloid.

3.2 Morphology

AFM micrographs of the pure PVA, PVA-Trp, PVA-Ag and PVA-AgTrp films are shown in Figure 3. The images are obtained in tapping mode. As can be seen, the morphology of the hybrid samples is different from that of the pure PVA. The most pronounced changes were observed in the case of PVA-AgTrp nanocomposite. The PVA films prepared from solution casting usually have low crystallinity [22]. Although PVA is in a glassy state at room temperature (glass transition temperature ~ 72 °C), the crystallization may occur in the later stage of film drying due to the plasticization effect of ambient humidity. The crystallization process usually results in the formation of dendrite or hedrite structures not sufficiently birefringent to be observed with cross-polarization microscopy [22]. As can be seen in Figure 3, AFM analysis of PVA in a tapping mode did not reveal the presence of any larger crystal formations. The morphologies of the PVA-Trp and PVA-Ag samples are different from that of the pure PVA but again no crystal formations were observed. In contrast, AFM images of the PVA-AgTrp sample

clearly show that functionalized nanoparticles act as nucleation centers for the growth of dendrite-like crystals. Similar crystal formations are noticed along the whole surface of the sample (the additional AFM images are given in [Supporting information](#), Figures S3). The results of the fluorescence microscopy study support the former conclusion. The fact that AgTrp nanoparticles are fluorescent implies that their distribution within the polymer matrix can be investigated by following the fluorescence signal.

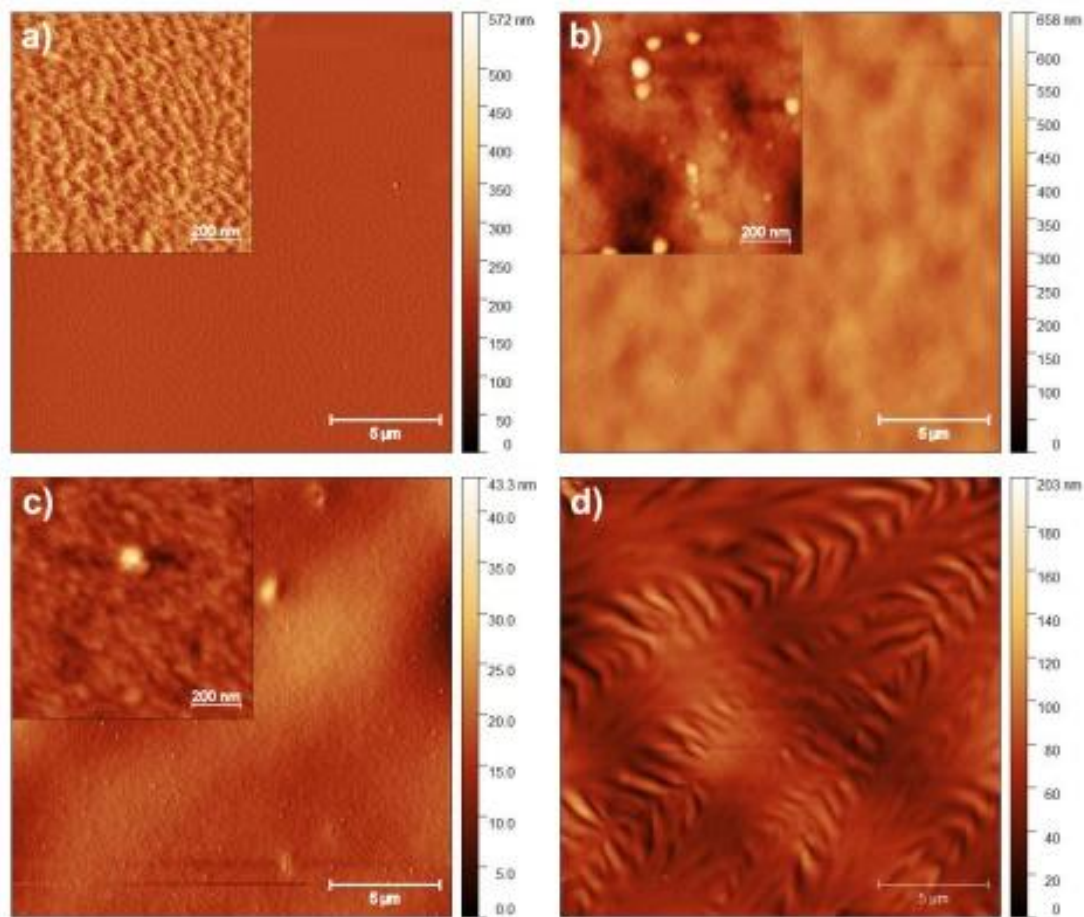


Figure 3. AFM topographic images of a) pure PVA, b) PVA-Ag, c) PVA-Trp and d) PVA/AgTrp films. The insets show higher resolution images.

The fluorescence microscopy results obtained for the pure PVA, PVA-Trp and PVA-AgTrp films are shown in Figure 4 (PVA-Ag films were non-fluorescent and they are excluded from the imaging study). For comparison, in Figure 4, we also present the corresponding visible images of the same samples. The visible image of the pure PVA film (Figure 4a) is relatively smooth, which is in agreement with AFM results (Figure 3 a) as well as with the literature data

[23]. Also, PVA film is non-fluorescent (Figure 4b). The microscopic images of PVA films that contain tryptophan (either free or attached to silver nanoparticles) show that the amino acid induces some morphological changes in the matrix material. This is particularly clear for PVA-AgTrp nanocomposite, where visible microscopy image (Figure 4e) depicts dendrite structures that resemble those detected by AFM (Figure 3d). The fluorescence microscopy images in Figures 4 d,f show that the additional structures observed in PVA-Trp and PVA-AgTrp samples indeed originate from the presence of the tryptophan. A strong fluorescence signal comes from the amorphous parts that surround the dendrites (Figure 4f), suggesting the areas where the hybrid AgTrp nanoparticles are situated.

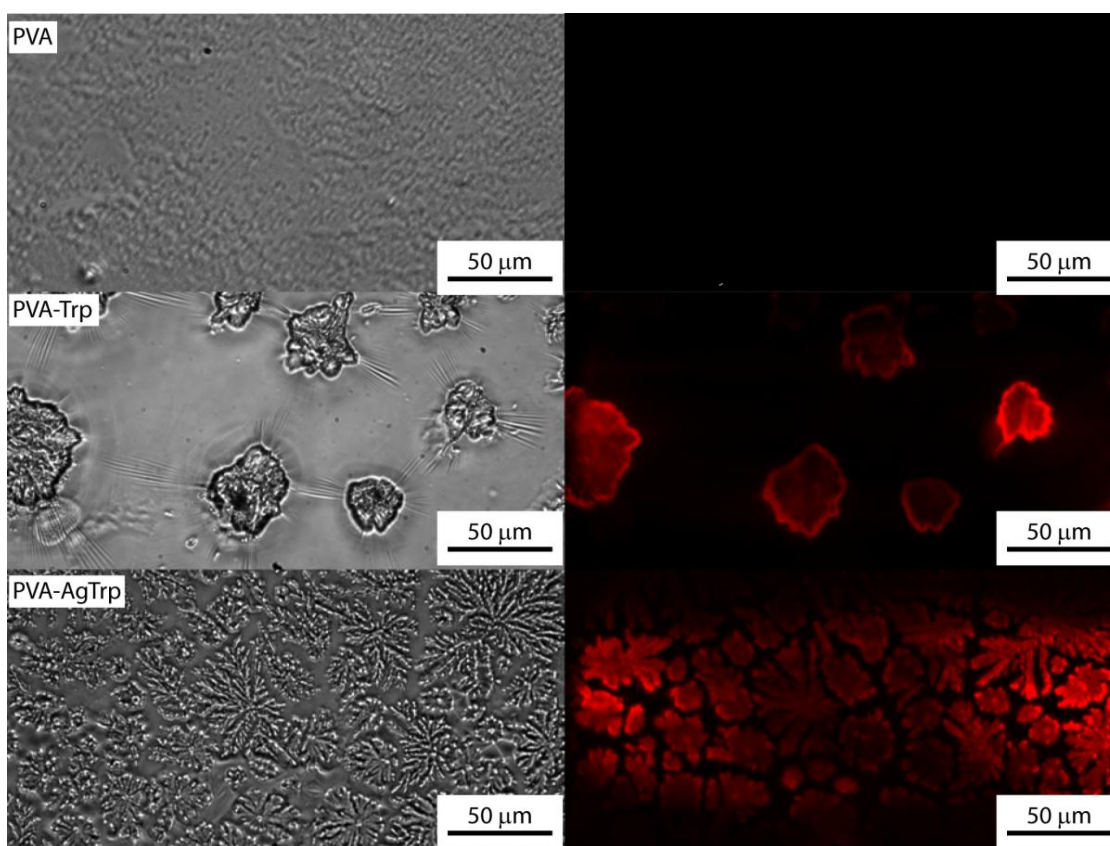


Figure 4. Bright-field and fluorescence images of the pure PVA a), b); PVA-Trp c), d) and PVA-AgTrp e), f) samples.

It should be noted that the fluorescence of the AgTrp hybrid nanoparticles strongly depends on the environment in which the particles are embedded [18]. A phase transfer of the AgTrp nanoparticles from polar (water) to non-polar (toluene) solvent resulted in a **~70 nm** shift of the fluorescence towards lower wavelength. For this reason, it is possible to determine the

polarity of the environments that surround the nanoparticles by detecting the position of the fluorescence emission. Based on this approach, we showed that the interaction of the AgTrp nanoparticles with *Escherichia coli* cells resulted in a strong increase in the fluorescence intensity [327–353 nm] range [18]. This spectral range corresponds to tryptophan emission in the non-polar environment (in this case the nanoparticles were mostly localized in the lipid bilayers of the cell membrane). At the same time, the autofluorescence of the cells in the [370–410 nm] range, which encompasses the tryptophan emission in a polar environment, remained unchanged. Since PVA contains polar OH groups, we decided to carry out the fluorescent imaging of the PVA-AgTrp nanocomposites in [327–353 nm] and [370–410 nm] ranges. In Figure 5a, we present a couple of flowerlike structural motives observed by visible microscopy of the PVA-AgTrp sample. The fluorescence microscopy images (Figure 5 b,c) obtained in [327–353 nm] and [370-410 nm] spectral windows, respectively, clearly suggest that the AgTrp nanoparticles are in the polar environment. There is no fluorescence in the [327–353 nm] range (Figure 5 b), while the fluorescence of the AgTrp nanoparticles in the [370–410 nm] range indicates that the nanoparticles are localized at the boundaries between the flowerlike structures and the amorphous phase of the polymer.

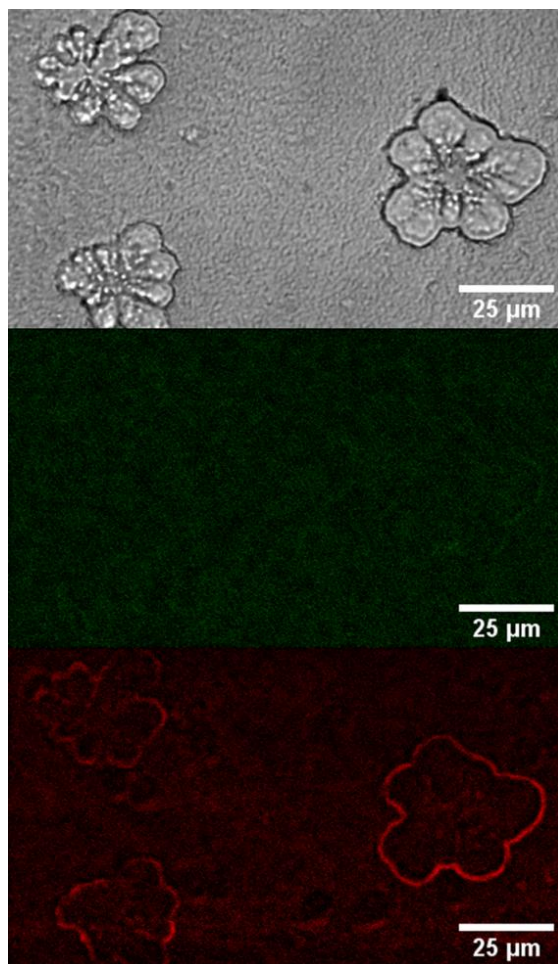


Figure 5. a) Bright-field image of PVA-AgTrp nanocomposite and fluorescence images of the same sample area obtained in b) [327–353 nm] and c) [370–410 nm] spectral ranges.

3.3. Thermal properties

Trp amino acid and AgTrp nanoparticles have profound effects on the thermal properties of the PVA matrix. Differential scanning calorimetry (DSC) heating scans of the PVA, PVA-Trp and PVA-AgTrp films are presented in Figure 6. DSC curves were split into two temperature regions to illustrate the changes in melting and glass transition behaviors. It can be seen that after the introduction of tryptophan and AgTrp nanoparticles there is a decrease in intensity of the melting peak and its shift towards lower temperature (Figure 6a). This, of course, implies that hybrid materials have lower crystallinities with respect to the pure polymer. Although the microscopy measurements show that tryptophan and AgTrp nanoparticles induce structural rearrangements of the matrix material, this is not reflected in the total contribution to the matrix crystallinity.

Also, a decrease in the melting temperature (usually reported as a position of the melting peak) suggests a decrease in the crystallite thickness. We believe that this is a result of a strong interaction of the polymer chains with tryptophan amino acid and AgTrp nanoparticles, which reduce their segmental mobility and, consequently, alleviate the plasticization effects of ambient humidity.

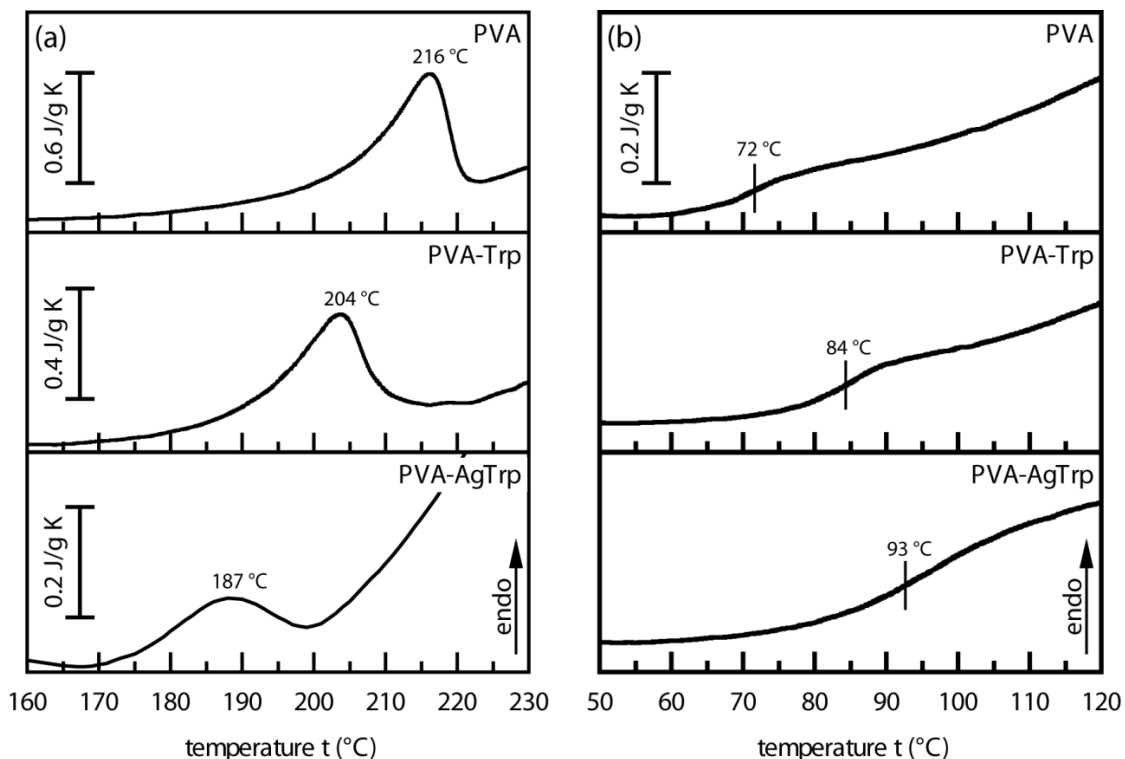


Figure 6. DSC heating curves of pure PVA, PVA-Trp and PVA-AgTrp films. For clarity, the curves are presented in the temperature ranges from a) 160 to 240 °C and b) 50-120 °C. (Heating rate: 20 °Cmin⁻¹).

This can be well seen in Figure 6b, which shows the glass transition region of three materials. PVA polymer exhibits a glass transition temperature of 72 °C (taken as a middle of the slope on the heat capacity curve). On the other hand, a dramatic increase in glass transition temperature to 84 and 93 °C was observed with the introduction of tryptophan amino acid and AgTrp nanoparticles, respectively. It should also be noticed that the shoulder on the heat capacity curves (e.g. the glass transition region) of the hybrid films is much broader than that of the pure PVA film. As we argued in our previous study [14], where similar effects of the bare silver nanoparticles on the PVA matrix were reported, this assumes changes in the distribution of segmental lengths that are activated during the heating. Glass transition is not a phase transition of second order in the strict sense, since the first derivative of the heat capacity curve over

temperature is a continuous function. Therefore the observed spreading of the glass transition region in hybrid materials means that tryptophan and AgTrp nanoparticles induce rearrangement of the chain segments in their vicinity leading to their activation in a much larger temperature range.

TGA measurements were carried out to investigate the effects of the tryptophan and the AgTrp nanoparticles on the thermal stability of the PVA matrix. Thermogravimetric curves of the pure PVA and hybrid films are shown in Figure 7.

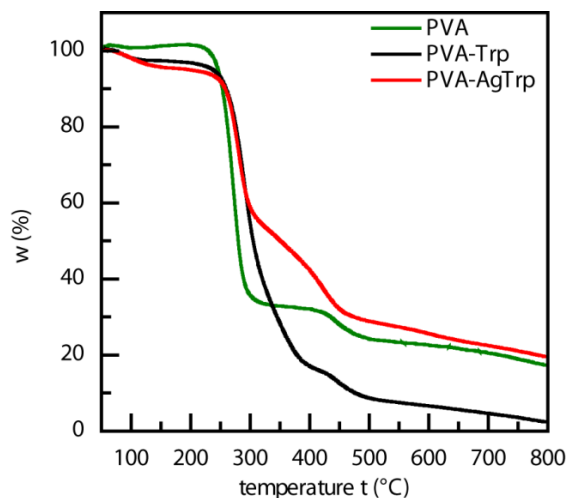


Figure 7. Thermogravimetric curves of PVA, PVA-Trp and PVA-AgTrp films obtained under nitrogen atmosphere. (Heating rate: $10\text{ }^{\circ}\text{Cmin}^{-1}$).

The TG curve of the pure PVA exhibits three distinct weight loss stages. The first stage that takes place at temperatures up to $150\text{ }^{\circ}\text{C}$ is attributed to the loss of the water [24]. The main weight loss processes occur in the temperature range $200\text{--}300\text{ }^{\circ}\text{C}$ and include the depolymerization and dehydration reactions [24,25]. However, dehydration reactions that lead to the formation of the polyene sequences (such as $-\text{CH}_2\text{-CHOH-CH}_2\text{-CHOH-}$ and $-\text{CH=CH-CH=CH-}$) are dominant in this stage. The third stage occurs between 350 and $450\text{ }^{\circ}\text{C}$ through intramolecular and Diels-Alder cyclization reactions of polyene sequences. The cyclization of polyenes results in the formation of benzene and other aromatic products, which provide a route for carbonization at high temperatures [24,25]. It can be seen in Figure 7 that both tryptophan and AgTrp nanoparticles affect the thermal degradation of the PVA matrix. The onset temperature of the main process of decomposition (stage 2) is slightly shifted towards higher temperatures. Also, tryptophan increases, while AgTrp nanoparticles shorten the second stage leading to, respectively, less and more carbonaceous residues at the end of the degradation

process (~800 °C). The AgTrp nanoparticles prevent to a certain extent the elimination (inter- or intra molecular dehydration) and chain-scission reactions, which in turn affect the decomposition route of the PVA chains and induces pronounced carbonization of the material. Similar effects were observed during the thermal degradation PVA-Ag nanocomposites [14].

Dielectric and photodielectric properties

Dielectric constant (ϵ') and dielectric loss (ϵ'') curves of the pure PVA, PVA-Trp, PVA-Ag and PVA-AgTrp films recorded in the dark as a function of frequency are shown in Figure 8. All four materials exhibit similar dependence of their dielectric constant toward frequency (Figure 8a). Dielectric constant decreases with the increase of frequency from 20 to 2×10^5 Hz. The obtained values for ϵ' of the pure PVA in this frequency range are in agreement with the dielectric spectroscopy results reported in the literature [26,27]. Figure 8a also shows that mixing of the pure tryptophan, as well as Ag and AgTrp nanoparticles with PVA, induce an increase in matrix dielectric constant in the whole range of measured frequencies. The strongest effect is observed after the introduction of the tryptophan (PVA-Trp sample), where the dielectric constant of the film is about ~75% higher than that of the pure PVA. Dielectric losses obtained for the pure PVA, PVA-Trp, PVA-Ag and PVA-AgTrp films are shown in Figure 8b. Due to interfacial polarization and conductivity effects, ϵ'' values are high at low frequencies and they decrease with increasing frequency (up to 10^4 Hz). At frequencies above 10^4 Hz, another process is observed in dielectric loss curves, usually associated with dipole relaxations [28].

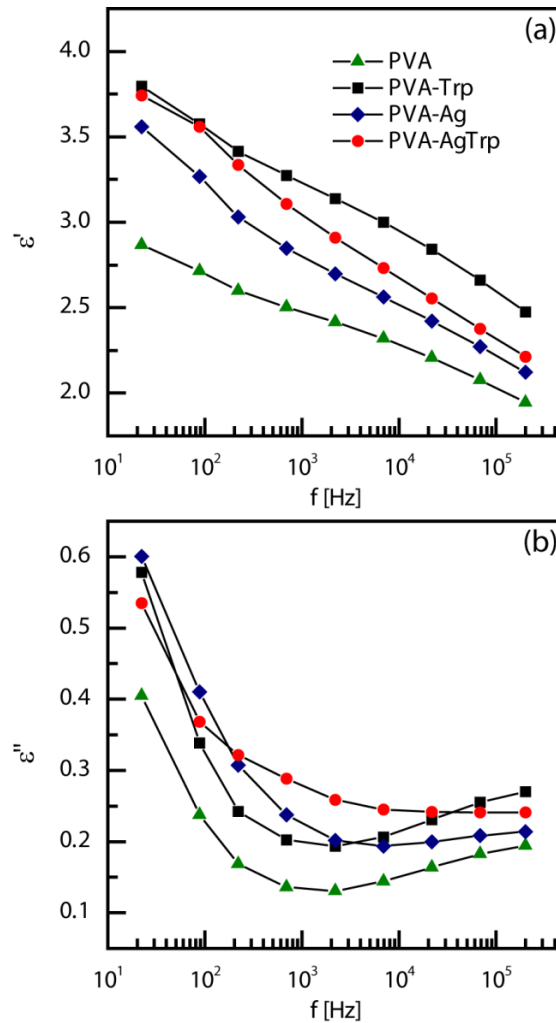


Figure 8. Bulk a) dielectric constant and b) dielectric loss vs. frequency for the pure PVA, PVA-Ag, PVA-AgTrp and PVA-Trp films. The measurements were performed at room temperature.

Taking into account that tryptophan, Ag and AgTrp nanoparticles are optically active materials, we were interested in the photodielectric properties of their hybrids with PVA. For practical reasons (the dielectric constant of the air was close to that of the thin polymer film) the photodielectric properties were investigated by surface measurements in an inert argon atmosphere. Also, due to interfacial polarization effects, the measurements at low frequencies up to 7 kHz were extremely sensitive to film drying upon illumination [29] leading to a significant scattering of data. On the other hand, above 7 kHz, the photodielectric behavior was fairly stable with high reproducibility and observable trends. For this reason, we decided to present the photodielectric results for high frequencies only. In order to increase the statistics, the photodielectric curves are recorded in 5 interchangeable dark-light steps each lasting for 25 s.

The samples were illuminated by using 250 nm and 385 nm light sources. The detailed measurement conditions were explained in the Experimental section. Figure 9 shows the relative changes of conductance (ΔG) and susceptance (ΔB) of PVA, PVA-Trp, PVA-Ag and PVA-AgTrp films during illumination with 250 nm photons (the samples are recorded at a constant frequency of 70 kHz). As can be seen, illumination induces a dramatic increase ($\sim 175\%$) in the conductance of the PVA-AgTrp sample. Susceptance is also affected by illumination but the relative changes are much smaller and there are no significant differences between the samples. The same types of measurements were performed by illumination of the samples with 385 nm light, at the wavelength of the resonant absorption of nanostructured silver (these results are included in [Supporting information](#), Figure S4).

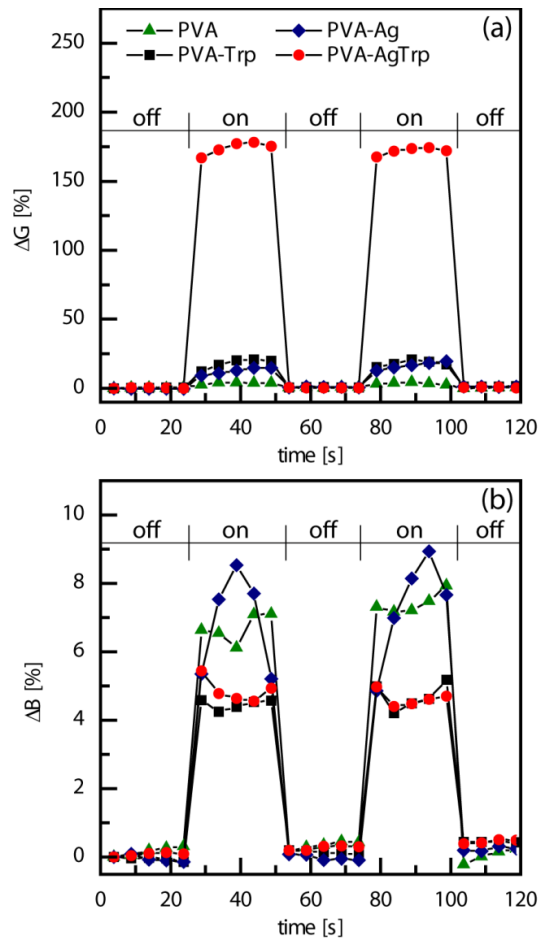


Figure 9. Time profiles of the relative changes in a) conductance (ΔG) and b) susceptance (ΔB) of the pure PVA, PVA-Ag, PVA-AgTrp (4) PVA-Trp films during photodielectric measurements at 70 kHz. The samples are illuminated with 250 nm light (light-off and light-on steps are indicated in the figure). The relative changes were calculated according to Eq. (1).

The effects of illumination on G and B of the samples were studied on various frequencies and their relative changes are shown in Figure 10. The results clearly show that illumination with 250 nm strongly affects the conductance of the PVA-AgTrp sample probably by increasing the number of free electrons when tryptophan is in an excited state. However, since the photoelectric responses of the PVA-Trp and PVA-Ag films are relatively weak (Figure 9a), it is obvious that the strong increase in conductance of PVA-AgTrp film is a consequence of the synergetic effects of tryptophan and Ag nanoparticles, when AgTrp hybrids are used as a filler for PVA.

We shall discuss the observed results considering Lewis's model for interfacial properties in polymer nanocomposites [30]. According to this model, the charges tend to accumulate on the particles surfaces due to differences in Fermi levels or chemical potentials of the particles and the host polymer. The charge accumulation at the surfaces, in turn, creates counter charges in the polymer chains at the interface layers. Finally, the Coulomb interaction of the charged particles induces the formation of an electrical double layer that consists of a Stern layer and a Gouy–Chapman diffused layer [30]. The later, diffused, layer contains trapped positive and negative ions and it influences the dielectric properties of the composite to a high extent [30]. Conduction via diffuse layers becomes increasingly important when the particles get closer together i.e. at higher particle contents in the composite. But, we believe that an increase in the number of electrons in the diffuse layers due to illumination of the AgTrp nanoparticles in the matrix can contribute to the observed increase in conductivity of the PVA-AgTrp film (Figures 9a and 10a). This effect will be less pronounced for 385 nm excitation since these photons do not have enough energy to excite the tryptophan molecule. As can be seen in Figure 10c, the illumination with 385 nm light induces a modest increase (between 5 and 20%) in conductance of PVA, PVA-Ag and PVA-AgTrp films. In contrast, the ΔG for the PVA-Trp sample upon illumination at 385 nm is negative or close to zero. The results in Figure 10c cannot be attributed to surface plasmon resonance effects having in mind that the pure PVA film is also affected by illumination. It may be a consequence of higher energy absorbed by the samples since Dökme *et al.* [31] showed that the dielectric permittivity of the Co-Ni doped PVA depended on the intensity of the incident light. At 385 nm, the irradiance was 4.4 mW/cm^2 , which was indeed higher than the irradiance of 1.3 mW/cm^2 when a 250 nm light source was used. This, however, does not explain why 385 nm light induces a decrease in conductance of PVA-Trp sample in the whole range of reported frequencies. Some other light-induced effects might also be involved.

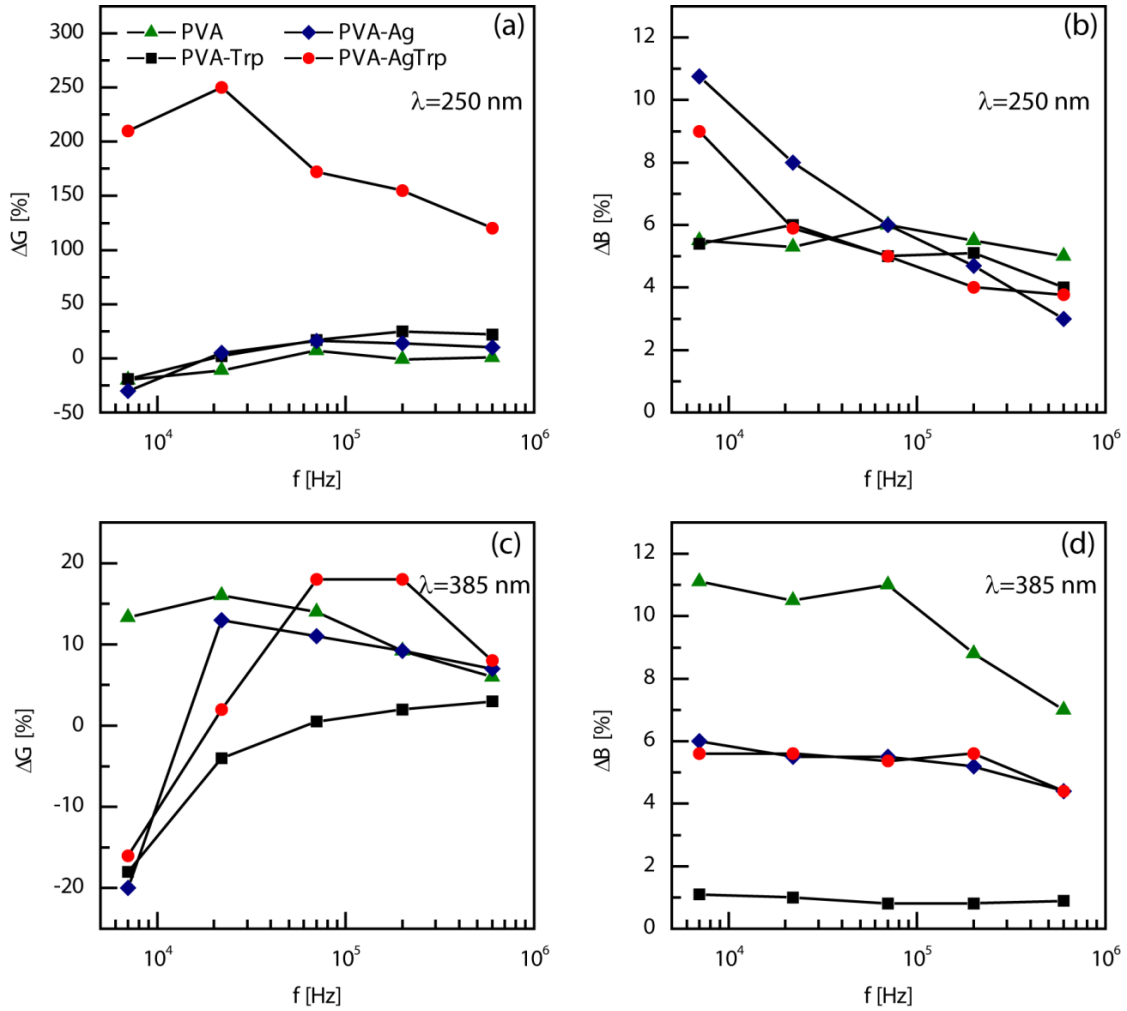


Figure 10. Photo-induced changes in conductance (ΔG) and susceptance (ΔB) of the pure PVA, PVA-Ag, PVA-AgTrp and PVA-Trp films at various frequencies. a) and b) after illumination with 250 nm light; c) and d) after illumination with 385 nm light. The relative changes were calculated according to Eq. (1).

Concerning relative changes in susceptance, 250 nm light affects differently silver containing samples, where a decrease in ΔB values with increase in frequency was observed, and PVA and PVA-Trp samples, where ΔB has more or less constant value of about ~5% regardless of measurement frequency (Figure 10b). Finally, Figure 10d shows that relative changes in susceptance during illumination with 385 nm light are the highest for the pure polymer. The relative changes in susceptance of PVA-Trp ($\Delta B \sim 1\%$), PVA-Ag ($\Delta B \sim 6\%$) and PVA-AgTrp ($\Delta B \sim 6\%$) are almost independent of frequency (Figure 10d).

Conclusion

The introduction of tryptophan functionalized silver nanoparticles (AgTrp) has profound effects on the properties of the PVA matrix. Bright-field and AFM microscopies showed that they induced changes in the morphology of the host polymer by acting as nucleation centers for the growth of dendrite-like structures. Tryptophan provides additional functionality to Ag nanoparticles, i.e. fluorescence, and, for this reason, it was possible to follow the distribution of the AgTrp hybrid nanostructures within the PVA by means of DUV fluorescence imaging. It was found that the AgTrp nanoparticles are mostly located at the boundaries of dendrite structures. The nanoparticles influence the thermal properties of the PVA matrix to a high extent. They reduce the crystallinity of the film and increase its glass transition temperature by ~ 20 °C. Also, they affect the thermal decomposition route of the PVA and induce pronounced carbonization of the material at the end of the thermal degradation process (~ 800 °C). Electric properties of the PVA-AgTrp nanocomposite films are strongly affected by the illumination with 250 nm light. During the illumination step, the relative increase in conductance (ΔG) for this sample was more than 200% at a measurement frequency of 22 kHz.

Acknowledgments

The research was funded by the Ministry of Education, Science and Technological Development of the Republic of Serbia. Deep UV imaging of hybrid PVA films was performed at the DISCO beamline of Synchrotron SOLEIL (France) as a part of research project no. 20120810. We acknowledge with gratitude the TNA support granted by Synchrotron SOLEIL.

1. M. Aslam, M. A. Kalyar, Z. A. Raza, Polyvinyl alcohol: a review of research status and use of polyvinyl alcohol based nanocomposites. *Polymer Engineering and Science* 58, 2119-2132 (2018)
2. A. Kausar, Innovations in poly(vinyl alcohol) derived nanomaterials. *Advances in Materials Science*, 20, No. 3(65), 2020
3. Z. W. Abdullah, Y. Dong, I. J. Davies, S. Barbhuiya, PVA, PVA blends, and their nanocomposites for biodegradable packaging application. *Polymer-Plastics Technology and Engineering*, 56, 1307-1344 (2017)

4. C. Saldías, S. Bonardd, C. Quezada, D. Radic, A. Leiva, The role of polymers in the synthesis of noble metal nanoparticles: a review. *Journal of Nanoscience and Nanotechnology* 17, 87-114 (2017).
5. L. Kool, A. Bunschoten, A. H. Velders, V. Saggiomo, Gold nanoparticles embedded in a polymer as a 3D-printable dichroic nanocomposite material. *Beilstein Journal of Nanotechnology*, 10, 442–447 (2019).
6. P. V. Gaikwad, S. K. Sharma, K. Sudarshan, V. Kumar, A. Kshirsagar, P. K. Pujari, Molecular packing of polyvinyl alcohol in PVA- gold nanoparticles composites and its role on thermo- mechanical properties. *Polymer Composites*, 39, 1137-1143 (2018)
7. B. Karthikeyan, Optical studies on thermally surface plasmon tuned Au, Ag and Au:Ag nanocomposite polymer films. *Spectrochim Acta A Mol Biomol Spectrosc*, 96, 456-460 (2012).
8. S. Mahendia, A. K. Tomar, P. K. Goyal, S. Kuma Tuning of refractive index of poly(vinyl alcohol): Effect of embedding Cu and Ag nanoparticles. *Journal of Applied Physics* 113, 073103 (2013)
9. A. M. Abdel Reheem, A. Atta, T. A. Afify, Optical and electrical properties of argon ion beam irradiated PVA/Ag nanocomposites. *Surface Review and Letters*, 24, 1750038 (2017)
10. S. Pandey, S. K. Pandey, V. Parashar, G. K. Mehrotra, A. C. Pandeya, Ag/PVA nanocomposites: optical and thermal dimensions. *Journal of Materials Chemistry*, 21, 17154-17159 (2011).
11. Synthesis, characterization, optical and antimicrobial studies of polyvinyl alcohol-silver nanocomposites. *Spectrochimica Acta Part A: Molecular and Biomolecular Spectroscopy*, 138, 434-440 (2015)
12. S. Mahendia, A. K. Tomar, P.K. Goyal, R. Kumar; S. Kumar, PVA-Ag nanocomposite: as glucose sensing material. 1st International Symposium on Physics and Technology of Sensors (ISPTS-1) Pune, India, IEEE Xplore, (2012)
13. R. Saikia, P. Gogoi, P. Datta Fabrication of Ag/PVA nanocomposites and their potential applicability as dielectric layer in thin film capacitor. *Journal of Experimental Nanoscience*, 8, 194–202, (2013)
14. Z. H. Mbhele, G. M. Salemane, C. G. C. E. van Sittert, J. M. Nedeljković, V. Djoković, A. S. Luyt, Fabrication and characterization of silver–poly(vinyl alcohol) nanocomposites, *Chemistry of Materials*, 15, 5019-5024 (2003)

15. U. K. Fatema, M. M. Rahman, M. R. Islam, M. Yousuf A. Mollah, Md. A. B. H. Susan Silver/poly(vinyl alcohol) nanocomposite film prepared using water in oil microemulsion for antibacterial applications. *Journal of Colloid and Interface Science*, 514, 648-655 (2018)
16. A. Celebioglu, Z. Aytac, O. C. O. Umu, A. Dana, T. Tekinaya, T. Uyar, One-step synthesis of size-tunable Ag nanoparticles incorporated in electrospun PVA/cyclodextrin nanofibers. *Carbohydrate Polymers*, 99, 808-816 (2014)
17. U. Divya Madhuri, V. Kesava Rao, E. Hariprasad, T. P. Radhakrishnan, In situ fabricated platinum—poly(vinyl alcohol) nanocomposite thin film: a highly reusable ‘dip catalyst’ for hydrogenation. *Materials Research Express*, 3, 045018 (2016)
18. R. Dojčilović, J. D. Pajović, D. K. Božanić, V. V. Vodnik, S. Dimitrijević-Branković, A. R. Milosavljević, S. Kaščakovà, M. Réfrégiers, V. Djoković, Functionalization of silver nanoparticles with tryptophan to probe the nanoparticle accumulation with single cell resolution. *Analyst*, 141, 1988–1996 (2016)
19. R. Dojčilović, J. D. Pajović, D. K. Božanić, Una Bogdanović, V. V. Vodnik, S. Dimitrijević-Branković, M. G. Miljković, Slavka Kaščakovà, M. Réfrégiers, V. Djoković, Interaction of amino acid-functionalized silver nanoparticles and *Candida albicans* polymorphs: A deep-UV fluorescence imaging study. *Colloids and Surfaces B: Biointerfaces* 155, 341–348 (2017)
20. D. K. Božanić, V. Djoković, J. Blanuša, P. Sreekumari Nair, M. K. Georges, T. Radhakrishnan, Preparation and properties of nano-sized Ag and Ag₂S particles in biopolymer matrix. *European Physical Journal E, Soft Matter* 22, 51–59 (2007).
21. L. Ambrosio, M. G. Verón, N. Silin, M. O. Prado, Synthesis and characterization of fluorescent PVA/PVAc-Rodhamine microspheres. *Materials Research*. 22, e20190133 (2019).
22. K. E. Strawhecker, E. Manias AFM of poly(vinyl alcohol) crystals next to an inorganic surface. *Macromolecules*, 34, 8475-8482 (2001).
23. J. Zhou, Y. Nishimura, A. Takasu, Y. Inai, T. Hirabayashi, Morphology and biodegradability of poly(ϵ -caprolactone)/poly(vinyl alcohol) block copolymers. *Polymer Journal*, 36, 695—704 (2004)
24. M. T. Taghizadeh, N. Yeganeh, M. Rezaei The investigation of thermal decomposition pathway and products of poly(vinyl alcohol) by TG-FTIR. *J. Appl. Polym. Sci.* 2015, Art No. 42117

25. J.-L. Shie, Y.-H. Chen, C.-Y. Chang, J.-P. Lin, D.-J. Lee, C.-H. Wu Thermal pyrolysis of poly(vinyl alcohol) and its major products. *Energy & Fuels* 2002, 16, 109-118.
26. J. Uddin, B. Chaudhuri, K. Pramanik, T. Ranjan Middy, B. Chaudhuri, Black tea leaf extract derived Ag nanoparticle-PVA composite film: Structural and dielectric properties. *Materials Science and Engineering B* 177 (2012) 1741–1747.
27. P. Lokanatha Reddy, K. Deshmukh, K. Chidambaram, M. M. Nazeer Ali, K. K. Sadasivuni, Y. R. Kumar, R. Lakshmi pathy, S. K. K. Pasha, Dielectric properties of polyvinyl alcohol (PVA) nanocomposites filled with green synthesized zinc sulphide (ZnS) nanoparticles. *J Mater Sci: Mater Electron*, 30, 4676–4687 (2019). <https://doi.org/10.1007/s10854-019-00761-y>
28. Y. Feng, W.L. Li, Y.F. Hou, Y. Yu, W.P. Cao, T.D. Zhang, W.D. Fei, Enhanced dielectric properties of PVDF-HFP/BaTiO₃-nanowire composites induced by interfacial polarization and wire-shape, *J. Mater. Chem. C*. 3 (2015) 1250–1260. <https://doi.org/10.1039/C4TC02183E>.
29. B Škipina, AS Luyt, L Csóka, V Djoković, D Dudić, Generation of photo charge in poly (ethyleneimine)-TiO₂-anthocyanin modified papers conditioned at different humidities. *Dyes and Pigments* 149, 51-58 (2018).
30. Pitsa, D.; Danikas, M. G. Interfaces features in polymer nanocomposites: A review of proposed models. *Nano*, 6, 497– 508 (2011). <https://doi.org/10.1142/S1793292011002949>
31. I. Dökme, D. E. Yildiz, S. Altindal, Illumination intensity effects on the dielectric properties of schottky devices with Co, Ni-doped PVA nanofibers as an interfacial layer. *Advances in Polymer Technology*, 31, 63-70 (2012).